

Time-dependent distributions in self-quenching nucleation

Vitaly A. Shneidman

Department of Physics, New Jersey Institute of Technology, Newark, New Jersey 07102, USA

(Received 5 July 2011; published 13 September 2011)

Diffusion- and interface-limited Becker-Döring (BD) -type nucleation is considered in a closed system, where supersaturation is depleted by growing nuclei. Special focus is on nonadiabatic effects, which become increasingly pronounced for barriers lower than $20\text{--}25k_B T$, and which lead to nucleation rates deviating from their quasi-steady-state (QSS) values. Several essential modifications of the QSS distribution are observed. For example, the front is continuous rather than sharp and has a double-exponential shape, which is in agreement with the earlier matched asymptotic solution obtained in neglect of depletion. The total number of nuclei is *larger* than predicted by the QSS approximation. The obtained distributions are compared with numerical solutions of the BD equations and can serve as initial conditions for further transition to the Ostwald Ripening stage.

DOI: [10.1103/PhysRevE.84.031602](https://doi.org/10.1103/PhysRevE.84.031602)

PACS number(s): 64.60.Q–

I. INTRODUCTION

The term “nucleation” is usually associated with the initial stage of a phase transformation in a sufficiently pure metastable system, when nuclei of a new phase are formed due to thermal fluctuations. The number and the diversity of applications is enormous [1]. The earliest, classical theory of nucleation [2–5] (see Sec. II) has a somewhat simplified view of the associated thermodynamics and kinetics but compensates for that by its potential to cope with very disparate time scales that appear in the problem. For a full self-contained picture of a phase transition, nucleation should be complemented by the effects of growing nuclei on the metastable phase, where one can identify two mainstream situations. First, the volume of the metastable phase can be diminished by growing and possibly overlapping nuclei, while the original level of metastability (supersaturation) remains unchanged. This corresponds to the Kolmogorov-Avrami scenario [6,7] with a huge number of metallurgical [8] and other applications. Second, the supersaturation can be exhausted by the growing nuclei, as in the Lifshits-Slyozov-Wagner (LSW) [9,10] description of Ostwald Ripening in supersaturated solutions (which has a direct analog in condensing vapors, etc.). Some formal similarities between the two type of effects can be established at small times since in this limit both linearly depend on the transformed mass; moreover, a different time scale notwithstanding, the Kolmogorov-type $\exp(-t^\alpha)$ time dependence of the nucleation rate remarkably appears as the first iteration in the depletion problem as well. The latter will be considered in the present study, leading to initial conditions for the LSW regime. The postnucleation transition to that regime requires much larger time scales and still remains an open problem [11].

Of main interest will be the distributions of growing nuclei over their sizes, which follow from the time-dependent Becker-Döring (BD) equation with a mass conservation law. Traditionally, such problems were solved using the quasi-steady-state (QSS) approximation, as described in the next section. Already in this approximation depletion of the metastable phase generally leads to a nonlinear integral equation, without a clear large parameter to enable a closed analytical solution. Iterative [12] and numerical [13] approaches were described for the interface- and the diffusion-limited growth, respectively, and in

appropriate limits the time and size can be rescaled to make the equation parameter free [13]. The QSS approximation leads to a convenient scaling and will serve as a reference point in the forthcoming analysis. At the same time, justification of the QSS approximation requires very high values of the nucleation barrier. This is not always true in real experiments, and almost never true in computer simulations, where barriers notably less than $20k_B T$ are a common practice. Thus, the focus of the study will be the non-QSS effects.

There are two aspects of such effects: those due to dependence of the nucleation flux on dimensionless rate \mathcal{N} of the barrier change [14,15] and those of transient nucleation following the “switch on” of nucleation at a given instant [15]; numerical studies are also available here—see, e.g., Ref. [1] and references therein. In neglect of depletion, both types of effects can be described using matched asymptotic (singular perturbation) technique and can be combined [16]. Depletion, however, adds nonlinearity to the problem, which enormously complicates asymptotic analysis, and further complications are added by the impossibility of integrating the growth equation analytically in the case of a time-dependent critical size. Nevertheless, the situation is not hopeless because of very large time scales associated with depletion. In particular, for a closed system \mathcal{N} remains small throughout most of the nucleation stage and can be neglected, while the changes of the critical size during that stage are minor, which allows an approximate analytical description of growth. A unified expression for the distribution function, which combines short-time transient and long-time depletion effects can then be constructed, as will be discussed below. Numerics will be used to assess the accuracy of the proposed approximations. It is possible to further increase the accuracy by combining analytical description of non-QSS nucleation with numerical description of growth. That would also allow us to broaden the picture of a phase transition beyond the nucleation stage, when the time dependence of the critical size becomes crucial. A separate discussion of a combined approach of that kind will be presented elsewhere.

The present paper has the following structure. In Sec. II the standard continuous nucleation equation and associated growth rates are introduced; basic assumptions regarding the two large parameters of the problem, the dimensionless barrier

B and the critical cluster number n_* , are discussed. Next, closing of the nucleation equation by the depletion condition is considered, and the iterative approach within the QSS approximation is described in some detail. Earlier relevant results on transient nucleation are also specified in this section.

Section III contains the main analytical results and their comparison with numerical solutions both for diffusion- and interface-limited nucleation and for growth. Appendix A gives explicitly the second iteration for the QSS approximation. While not used explicitly, except for the figures, this iteration helps us to understand the limits of accuracy of the treatment. Numerics is described in Appendix B. It is based on a generalization of the Turnbull-Fisher version of the discrete BD equation, which is expected to be very close to continuous approximation for a sufficiently large critical number.

II. BACKGROUND

A. The nucleation equation

The classical thermodynamics of nucleation was developed by Gibbs, who showed that the minimal work $W(R)$ required to form a nucleus of radius R in a supersaturated medium passes through a maximum $W_* \equiv W(R_*)$ at the critical radius R_* , the same as introduced by Kelvin. The value W_* determines the dimensionless nucleation barrier $B = W_*/k_B T$ and, according to Volmer and Weber [2], determines the exponential part of the nucleation rate $J \propto e^{-B}$ (see, e.g., Ref. [17] for a textbook description of nucleation thermodynamics). Kinetics of nucleation was further considered by Farkas [3], Becker and Döring [4] (BD), and Zeldovich [5], who treated it as a random walk in the n -space, n being the number of monomers in a nucleus (for simplicity of notation, $n = R^3$ with dimensionless R will be used). The corresponding discrete Master Equation for the distribution of nuclei $f_n(t)$ is known as the “BD equation”; see Appendix B. In the case of small supersaturations a continuous Fokker-Plank equation can be written:

$$\frac{\partial f}{\partial t} = -\frac{\partial j}{\partial R}, \quad j = -\beta \frac{\partial f}{\partial R} + \dot{R} f \quad (1)$$

with $f(R, t) = f_n(t) dn/dR$. The deterministic growth rate \dot{R} follows from macroscopic (hydrodynamic) description of kinetics of a single nucleus, while the diffusivity $\beta(R)$ is determined by an “Einstein relation” in the R space [5]:

$$\beta = -\frac{k_B T \dot{R}}{dW/dR}. \quad (2)$$

Boundary conditions (BCs) are selected as follows. At small $R \ll R_*$ a quasi-equilibrium distribution $f^{\text{eq}}(R) \propto \exp[-W(R)/k_B T] dn/dR$ is expected; at large R nuclei just grow, implying either a drift flux $j \rightarrow \dot{R} f$ or a vanishing reduced distribution $f/f^{\text{eq}} \rightarrow 0$. Such BCs allow a steady-state solution with an R -independent flux, given for $W_* \gg k_B T$ by [5]

$$J = \frac{\Delta}{2\tau\sqrt{\pi}} f^{\text{eq}}(R_*), \quad \Delta^{-2} = -\frac{1}{2k_B T} \frac{d^2 W}{dR^2} \Big|_{R=R_*}, \quad (3)$$

$$\tau^{-1} = \frac{d\dot{R}}{dR} \Big|_{R=R_*}.$$

This will be further used as QSS or “Zeldovich” nucleation rate.

A related textbook [18] introduces nucleation kinetics specifically for diffusion-limited growth, which will be considered in the present study. In this case one has

$$\dot{R} = \frac{R_*^{\theta+1}}{R^\theta \tau} \left(1 - \frac{R_*}{R}\right), \quad (4)$$

where $\theta = 1$ and the time scale τ is related to diffusion coefficient in the medium. Similarly, the other mainstream model considers free molecular (“ballistic”) interface-limited growth and for small supersaturations corresponds to $\theta = 0$ in the above expression. In that case τ is related to molecular collision frequency, as studied by Hertz and Knudsen.

For work W a standard expression, often known as the “droplet model,” will be used:

$$W(R) = R^2 \sigma - \Delta \mu n, \quad (5)$$

where σ is “interfacial tension” (properly scaled to account for dimensionless $R = n^{1/3}$), while $\Delta \mu > 0$ is the difference of chemical potentials. In the vapor-to-liquid transition

$$\Delta \mu = k_B T \ln S, \quad (6)$$

where $S > 1$ is supersaturation, and the ideal gas equation of state is used for vapor. For small S close to 1, which are implied in the present study, a similar expression holds for supersaturated solutions. With these specifications one has

$$R_* = \frac{2}{3} \frac{\sigma}{k_B T \ln S}, \quad W_* = \frac{4}{27} \frac{\sigma^3}{(k_B T \ln S)^2}. \quad (7)$$

Apart from the time scale τ , Eqs. (1) and (4) with $\beta \propto 1/R^{\theta+2}$ are thus fully specified by two independent dimensionless parameters $\sigma/k_B T$ and $\ln S$. Equivalently, one can use another dimensionless pair $B = W_*/k_B T$ and $n_* = R_*^3$ with

$$\sigma/k_B T = 3B/n_*^{2/3}, \quad \ln S = 2B/n_*$$

and with expected

$$n_* \gg B \gg 1. \quad (8)$$

In the above, the condition $B \gg 1$ is needed for singular perturbation analysis of Eq. (1) at small times, in the transient regime [15]. The large $n_* \gg B$ is required to justify the continuous approximation and occasionally will be used for linearization of $\ln S \simeq S - 1$. (Otherwise, unlike the former condition $B \gg 1$, the requirement of a large critical number is nonessential for the BD picture, as long as one uses its discrete version with correspondingly adjusted \dot{R} and postulates the validity of the droplet model at the smallest sizes. The stationary Zeldovich formula remains reasonably accurate even for n_* of several units [19]; the aforementioned transient solution in a general form is valid for $n_* \gtrsim B$, while the strong inequality $n_* \gg B$ leads to the simplest growth rate (4) with an elementary expression for the “incubation time”; see Sec. IID.) No special hierarchy between B and $n_*^{2/3}$ is expected in the present study, although large values of dimensionless interfacial tension $\sigma/k_B T$ reduce the contributions of small clusters (see below) and help to justify the ideal gas approximation in the equation of state. It is also

assumed that while B and n_* change in time together with the supersaturation, the ratio $B/n_*^{2/3}$ remains fixed together with T and σ . Additional restrictions on the relation between B and n_* will be introduced in connection with depletion effects.

B. Depletion of monomers

It is more convenient to start with the discrete BD equation. One could formally write conservation of mass [20]

$$f_1 + \sum_{n=2}^{\infty} n f_n = \text{const} \tag{9}$$

and use this to determine the number of monomers $f_1(t)$, which in turn determines the supersaturation. In particular, with this closure the BD equation predicts [20] the emergence of the LSW asymptotic regime [9,10] in the limit $t \rightarrow \infty$ when the sum is dominated by very large n . At smaller, nucleation time scales, however, one notes the potential contribution of small clusters: dimers, trimers, etc. At those sizes the macroscopic droplet model used to evaluate $W(R)$ breaks down, as already noted by Farkas [3]. It is also unclear that it is consistent to include contributions of such clusters in the conservation law, at the same time ignoring them in the ideal-gas-type equation of state used to evaluate $\Delta\mu$.

In order to avoid the above difficulties, one can replace the lower summation limit by some “mesoscopic” cluster size n_0 . This highlights the asymptotic nature of the problem associated with consumption of monomers by large droplets with $n \gg 1$ and allows one to avoid a discussion of the delicate questions associated with properties of the metastable phase on the microscopic level. The procedure is consistent as long as the actual selection of n_0 does not matter, which can be verified operationally. Once the smallest n are excluded, the sum can be replaced by an integral. In R variables with $R_0 = n_0^{1/3}$ one has

$$\Omega_3(t) = \int_{R_0}^{\infty} R^3 f(r,t) dR \tag{10}$$

for the total “mass” contained in droplets. If f is normalized per monomer of the metastable phase one can write

$$S(t) = S_0[1 - \Omega_3(t)]. \tag{11}$$

The above relation will be used in both numerical and analytical parts of the study. In the former, the value of R_0 is selected in the growth region, somewhat above the initial critical size R_*^0 , and insensitivity of the results to the actual value of the selection is verified. Analytically, only terms that formally unboundedly grow at large t , and that are explicitly insensitive to the lower limit of integration in Eq. (10), will be considered.

Once the time dependence of the supersaturation is established, it can be used to relate the barrier and the critical cluster number to their initial values:

$$B(t) = B_0 \left(\frac{\ln S_0}{\ln S} \right)^2, \quad n_*(t) = n_*^0 \left(\frac{\ln S_0}{\ln S} \right)^3. \tag{12}$$

Note that as long as $\Omega_3(t)$ remains small, one can use the so-called nucleation theorem (or, in our case simply the relation $dB/d \ln S = n_*$) to write for large n_*^0

$$J(t) \simeq J_0 \exp[-n_*^0 \Omega_3(t)]. \tag{13}$$

This definition of the “nucleation curve” $J(t)$ can be used in both QSS and non-QSS cases, which differ in the way $\Omega_3(t)$ is evaluated. In non-QSS situation, however, $J(t)$ does not directly correspond to a “nucleation rate.”

C. The QSS approximation

To further simplify notations, let us agree to understand “ t ” in the following analytical part of the study as the dimensionless “time”:

$$\int_0^t dt'/\tau(t') \simeq t/\tau_0. \tag{14}$$

The earlier rate J is then multiplied by τ , eliminating the latter from the preexponential. A scaled radius $r = R/R_*^0$ also will be used.

In the QSS approximation—indicated by a superscript q —it is assumed that, in addition to QSS rate J , nuclei also have negligible initial size $r = 0$ and that they evolve with a bulk growth rate \dot{r}^q neglecting the curvature effects:

$$\dot{r}^q = \frac{1}{r^\theta} \left(\frac{R_*(t)}{R_*^0} \right)^{\theta+1} \tag{15}$$

(all three assumptions are consistent with each other, and are either satisfied or violated simultaneously [21]). Neglecting the weak time dependence of the critical size during the nucleation stage, one can integrate the growth equation to obtain

$$r^q(t) \simeq [(\theta + 1)t]^{1/(\theta+1)}, \tag{16}$$

which gives

$$\Omega_3^q(t) = n_*^0 \int_0^t dt' J(t') r^q(t-t')^3 \approx \frac{1}{\theta + 4} J_0 n_*^0 r^q(t)^{\theta+4}. \tag{17}$$

In the above, the approximation indicates the first iteration. Introducing a time scale

$$\tilde{t} = \frac{1}{\theta + 1} \left(\frac{\theta + 4}{J_0 (n_*^0)^2} \right)^{(\theta+1)/(\theta+4)}, \tag{18}$$

one has

$$J^q(t) \approx J_0 \exp[-(t/\tilde{t})^\alpha], \quad \alpha = \frac{\theta + 4}{\theta + 1}. \tag{19}$$

This approximation is shown by a solid line in the left-hand sides of Fig. 1 for $\theta = 1$ and Fig. 2 for $\theta = 0$, respectively. The area under such lines is given by $\omega_0^q = \Gamma[(2\theta + 5)/(\theta + 4)]$, which evaluates to $\omega_0^q \approx 0.887$ for $\theta = 1$ and to $\omega_0^q \approx 0.906$ for $\theta = 0$, in accord with Refs. [6,12]. The total number of nuclei is then $\Omega_0 = J_0 \tilde{t} \omega_0$.

Second iterations are given in the Appendix A. For $\theta = 1$ this iteration is shown by a dashed line in the same left part of Fig. 1 with $\omega_0^q \simeq 0.9316$; this already provides sufficient accuracy compared to the available numerical solution of the corresponding integral equation [13] (a somewhat different

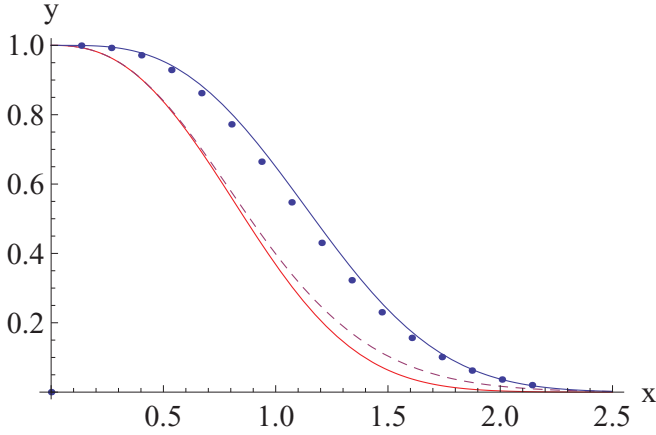


FIG. 1. (Color online) The scaled Zeldovich rate $y = J/J_0$ as a function of “time” $x = t/\tilde{t}$ in diffusion limited case. Symbols: numerical solutions of Becker-Döring equations with $B_0 = 25$ and $n_*^0 = 216$; solid line on right: Eqs. (13) and (29) with $\theta = 1$. The solid and dashed lines on left are the QSS approximation in the first two iterations: $\exp(-x^{5/2})$ and Eq. (A1), respectively.

scaling used in the present work should be mentioned). For $\theta = 0$ changes introduced by the second iteration are minor [12]. One has $\omega_0^q \simeq 0.910$, and the corresponding curve blends in with the one representing the first iteration in the left part of Fig. 2 with the difference less than 0.01.

Note that in the absence of a large parameter, the convergence rate of the iterative approach is determined by the power index α in Eq. (19). For large α the corresponding rate approaches $J_0\Theta(\tilde{t} - t)$, and already the first iteration is rather accurate, as for interface-limited growth with $\alpha = 4$. In the diffusion-limited case a smaller value of $\alpha = 5/2$ leads to a more substantial contribution of the second iteration. Nevertheless, the resulting deviation is still minor, and the much more compact first iteration will serve as a starting point for the forthcoming study of non-QSS effects. Obviously, the

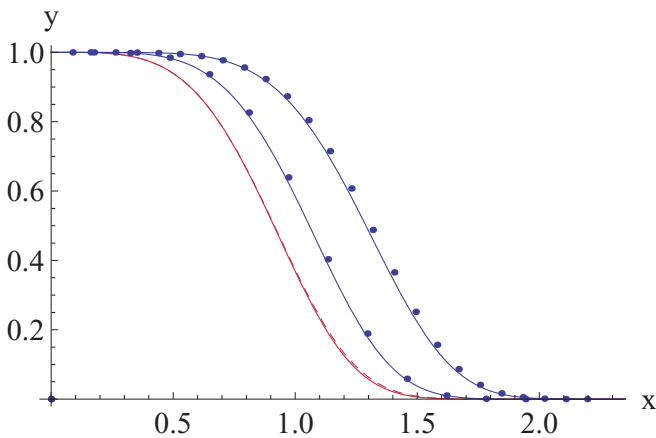


FIG. 2. (Color online) Same as in Fig. 1, but for the ballistic model with $\theta = 0$. Symbols: numerical solutions of BD equations with $B_0 = 25$ (right) and $B_0 = 30$ (left); the two lines on right: Eqs. (13) and (29) for the same parameters. The solid line on left is $\exp(-x^4)$, the first iteration in the QSS approximation; the second QSS iteration (dashed) gives a visually indistinguishable result.

latter must exceed the aforementioned deviation in order for the treatment to make sense.

Within the QSS approximation accuracy can be somewhat improved by an account for variable parameters τ and R_* when evaluating the dimensionless time and $r^q(t)$, and by using a more accurate approximation in the exponential of Eq. (13) for smaller n_*^0 . In addition, for $\theta = 0$ an “exact” (in the QSS sense) system of ordinary differential equations for the four lower moments $\Omega_0 - \Omega_3$ [22] can be integrated numerically. However, for the parameters considered there are no visible changes in the nucleation curve. In particular, the area ω_0^q changes from 0.904 for $B_0 = 20$ to 0.907 for $B_0 = 40$. In practice, corrections to the Kolmogorov’s $\exp(-t^4)$ law become detectable at much smaller B_0 , when the QSS approximation itself is not justified.

Evaluation of the QSS distribution is straightforward. Introducing the growth time

$$t_{gr}^q(r) \simeq \frac{1}{\theta + 1} r^{\theta+1}, \quad (20)$$

one relates the distribution at any time to the nucleation curve $J^q(t)$ as

$$f^q(r, t) = \frac{1}{r^q} J^q[t - t_{gr}^q(r)] \Theta[t - t_{gr}^q(r)]. \quad (21)$$

Typical examples are shown by right-most dashed lines in Figs. 3 and 4 and appear in agreement with similar curves presented, e.g., in Ref. [13].

Using n_*/\sqrt{B} as an estimation of the preexponential of the dimensionless nucleation rate, one can now complement the chain of inequalities (8) by the condition

$$B + \frac{1}{2} \ln B - 3 \ln n_* \gg 1,$$

which appears in connection with depletion. This condition ensures that nucleation is not too fast, so that the lifetime of the metastable state \tilde{t} is sufficiently long. A very strong inequality here would justify the QSS approximation with

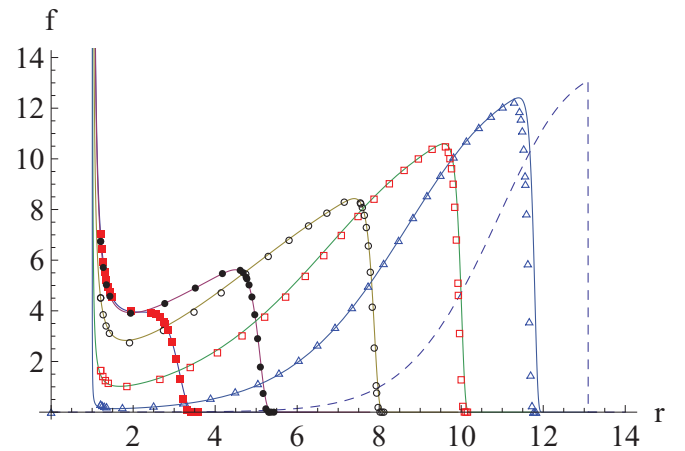


FIG. 3. (Color online) Scaled distributions $f(r, t)/J_0$ for $r > 1$ at different times t (diffusion). From left to right, according to the front position: $t = 5000, 10000, 20000, 30000$, and 40000 (in original time units with $\tau_0 \simeq 466.6$ and $\tilde{t} \simeq 18680$). Solid lines: Eq. (32); symbols: from Becker-Döring equations (numerics). Dashed line: the QSS approximation at $t = 40000$.

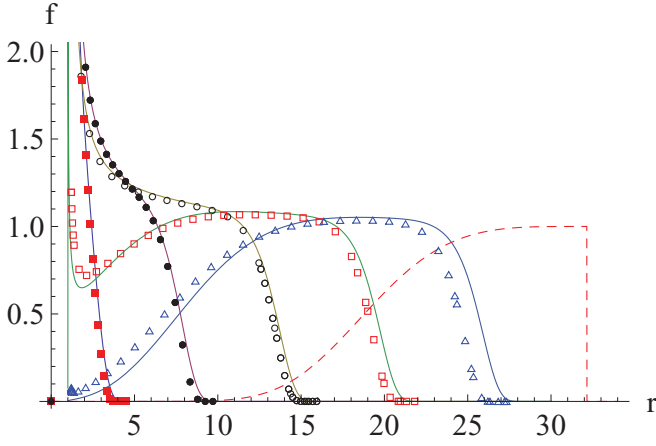


FIG. 4. (Color online) Scaled distributions $f(r,t)/J_0$ for $r > 1$ at different times t (ballistic). From left to right, according to the front position: $t = 500, 1000, 1500, 2000, 2500$ (in original time units with $\tau_0 \simeq 77.8$ and $\tilde{t} \simeq 1138$). Solid lines: Eq. (32); symbols: from BD equations (numerics). Dashed line: the QSS approximation at $t = 2500$.

nuclei significantly exceeding the critical size contributing to depletion. Conversely, a strong violation of this inequality would imply an almost immediate termination of nucleation due to consumption of monomers by smaller clusters, without a clear separation of the nucleation and the growth regions. It is assumed in the following discussion that while the condition $B - 3 \ln n_* \gg 1$ holds and average nuclei depleting the system are well in excess of the critical size, the inequality is not strong enough to neglect the non-QSS effects.

D. Transient distributions in neglect of depletion

The singular perturbation solution to the BD equation was obtained in Ref. [15] using a combination of matched asymptotic and Laplace transformation techniques. The transient nucleation flux—the “nucleation rate”—was shown to have a universal double-exponential shape, but with parameters sensitive to the deterministic rate \dot{r} associated with a selected form of the BD equation. In Ref. [23] the general solution was extended toward arbitrary large sizes in the growth region (in neglect of depletion) and was specified for several mainstream nucleation models, including the diffusion- and interface-limited cases, which are of interest in the present study. One has in present notations [15]

$$j(r,t) = J_0 \exp\{-\exp[t_i(r) - t]\} \quad (22)$$

with the “incubation times” $t_i(r)$ expressed in terms of decay and growth integrals $\pm \int dr/\dot{r}$ [23]. In case of small supersaturations with $\dot{r} = (1 - 1/r)r^{-\theta}$ the integrals are elementary for $\theta = 1$ and 0, and the incubation time is given by

$$t_i^{\text{Dif}}(r) = \ln(6B_0) + \frac{1}{2}(r-1)^2 + 2(r-1) + \ln(r-1) - \frac{3}{2}, \quad (23)$$

$$t_i^{\text{Bal}}(r) = \ln(6B_0) + r + \ln(r-1) - 2 \quad (24)$$

[which are, respectively, Eqs. (11) and (12) in Ref. [23]].

The distributions in the growth region are related to fluxes by

$$f(r,t) = \frac{1}{\dot{r}} j(r,t). \quad (25)$$

For $\theta = 1$ they are illustrated by the two left curves in Fig. 3 [the figure includes the depletion effects (see below), but at the two smallest times those are negligible]. The distributions are singular near $r = 1$ and develop a stationary minimum near $r = 2$ at $t \gtrsim \ln(6eB_0)$. In contrast, in the ballistic case $\theta = 0$ transient distributions are monotonic; see the three left small-time curves in Fig. 4.

III. RESULTS

A. The nucleation curve

The above transient distributions are characterized by a narrow front of double-exponential shape, which propagates in the r space with a rate \dot{r} . For the location of the front $r_i(t)$ we use the condition [24]

$$t_i(r_i) = t. \quad (26)$$

Unlike the case of interface limited growth (see below), in the diffusion-limited situation the above equation cannot be solved exactly and will be treated numerically. Connection with the QSS counterpart given by $r^q(t)$ follows from the large-time asymptote

$$r_i^{\text{Dif}}(t) \sim r^q(t) - 1 - \frac{1}{2\sqrt{2t}} [\ln(72B_0^2 t) + 1]. \quad (27)$$

In the ballistic case, on the other hand, one can write explicitly [24]

$$r_i^{\text{Bal}}(t) = 1 + \mathbf{W}\left[\frac{e^{1+t}}{6B_0}\right] \sim r^q(t) - \ln \frac{6B_0 t}{e^2}, \quad (28)$$

where $\mathbf{W}[z]$ is the so-called Lambert W function, defined as the root of $z = \mathbf{W}e^{\mathbf{W}}$.

Obviously, there is a certain flexibility in the precise definition of the “front” within the finite transition layer, and, alternatively, one could define it from the “time lag” $t_i + \gamma$ [with $\gamma = 0.5772\dots$ being the Euler constant [23]], i.e., from an equation

$$t_i(r_i) + \gamma = t.$$

This would somewhat increase the accuracy when estimating the transformed mass due to a correct account for the shape of the transition layer (see also Ref. [25] for a similar issue in the Kolmogorov-Avrami problem). However, at least for the parameters considered no overall improvement of accuracy was observed, and the slightly simpler definition of $r_i(t)$ given by Eq. (26) will be used.

At large times, analogously to the first iteration in the QSS approximation, one can write

$$\Omega_3(t) \approx \frac{1}{\theta + 4} J_0 n_*^0 r_i(t)^{\theta+4}. \quad (29)$$

This determines the nucleation curve via Eq. (13), as shown in Figs. 1 and 2 by solid lines on right. Results are in agreement with numerical solutions of the BD equation, represented by symbols. The deviation from corresponding QSS curves

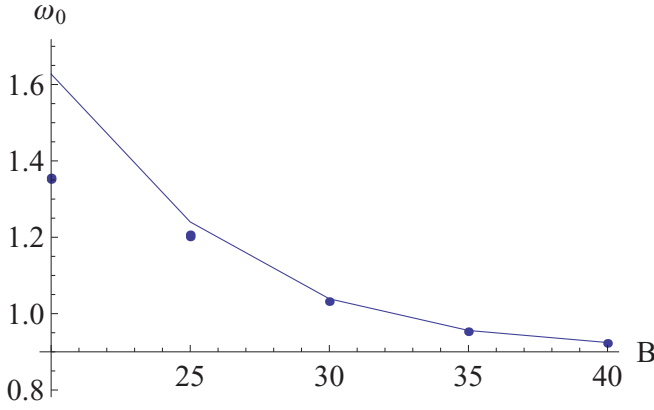


FIG. 5. (Color online) The scaled number of nuclei $\omega_0 = \Omega_0/J_0\tilde{t}$ as a function of dimensionless initial barrier $B = B_0$ (ballistic model). Note the excess over the QSS “Kolmogorov” value $\omega_0^q \simeq 0.9$. Line: from Eq. (30), with $\omega_0 - \omega_0^q \approx \omega_0^q \ln(B_0\tilde{t})/\tilde{t}$ at large B_0 . Symbols: from BD equations (numerics).

decreases with the increase of the barrier, and for $B_0 \simeq 40$ (not shown) would practically disappear.

The total number of nuclei can be evaluated as

$$\Omega_0 \simeq \int_0^\infty dt J(t) - \gamma J_0. \quad (30)$$

The last term describes the reduction of the number of nuclei due to transient nucleation at small t . That contribution, however, is minor compared to the broadening of the nucleation curve $J(t)$ versus $J^q(t)$. Thus, somewhat unexpectedly the numbers of nuclei are increased compared to the QSS approximation, as further emphasized in Fig. 5.

To estimate the effect, note that in both QSS and non-QSS approximations the Zeldovich rate J departs from its original value J_0 at comparable values of Ω_3 . Thus, if $t^q \lesssim \tilde{t}$ is the characteristic time when the QSS nucleation curve is still flat, the non-QSS counterpart of this time, t , is determined by the condition $r^q(t^q) \approx r_i(t)$, where large-time asymptotic approximation for $r_i(t)$ can be used. The extra number of nuclei is then estimated as $\delta\Omega_0 \approx J_0(t - t^q)$, which should be compared to $\Omega_0^q = \omega_0^q J_0\tilde{t}$. In both models ω_0^q is not far from 1, so that one obtains $\delta\Omega_0/\Omega_0^q \sim [\sqrt{2\tilde{t}} + (1/2)\ln(72eB_0^2\tilde{t})]/\tilde{t}$ in the diffusion-limited case and $\sim \ln(B_0\tilde{t})/\tilde{t}$ in the ballistic case, respectively. Neglecting the weak logarithmic dependence on the barrier, one expects that for each of the two models the non-QSS effects scale with \tilde{t} , which in turn is a power of $J_0(n_*^0)^2$. Using $J_0 \simeq (1/2)\sqrt{3/(\pi B_0)}n_*^0 \exp(-B_0)$, one thus expects approximately similar values of \tilde{t} for different initial conditions if the parameter

$$B_0 - 3 \ln n_*^0$$

is held fixed. While the non-QSS corrections to Ω_0 are generally not too large, for a moderate barrier (or large critical size) they can nevertheless significantly exceed the minor difference between the first and second QSS iterations, which justifies using the former in the non-QSS case.

B. The distribution function

Consider some small value of $r_0 > 1$ as “initial size for growth” and treat the flux $j(r_0, t)$ as the “nucleation rate.” Using a distinct separation of the transient and depletion time scales, one can approximate this flux as

$$j(r_0, t) \approx J(t) \exp\{-\exp[t_i(r_0) - t]\}. \quad (31)$$

Strictly speaking, this flux is also affected by the rate of the change of the barrier [14–16], but this rate is small during most of the nucleation process due to large \tilde{t} and will be ignored.

As long as the time dependence of R_* can be neglected, the distribution $f(r, t)$ at size r is determined by the flux $j(r_0, t')$ evaluated at the “retarded” time $t' = t - t_{gr}(r, r_0)$ with $t_{gr}(r, r_0) = \int_{r_0}^r dr/\dot{r}$. Shifting of $t_i(r_0)$ by $t_{gr}(r, r_0)$ just turns the former into $t_i(r)$ for any selection of r_0 . However, by selecting r_0 sufficiently close to 1 one also can require $t_{gr}(r, r_0) = t_i(r)$, which is possible to achieve due to insensitivity of $J(t)$ to changes of the argument, which are small compared to \tilde{t} . Within a reasonable range, other selections of r_0 can be discussed, but the suggested choice leads to the most compact expression for the distribution

$$f(r, t) \approx \frac{r^{\theta+1}}{r-1} J[t - t_i(r)] \exp\{-\exp[t_i(r) - t]\}. \quad (32)$$

The nucleation curve $J(t)$ is determined by Eqs. (13) and (29) for $t \geq 0$ and is defined as $J(t) \equiv J_0$ for $t < 0$. The incubation time $t_i(r)$ for the diffusion ($\theta = 1$) and the ballistic ($\theta = 0$) models is given by Eqs. (23) and (24), respectively.

Equation (32) is the main result of the present work; Figs. 3 and 4 give typical illustrations together with numerical data. The largest time considered was about $2\tilde{t}$. The proposed analytical approximation is reasonably accurate during most of the nucleation period; the accuracy is somewhat less than the one observed for the nucleation curves due to additional simplifying assumptions when describing growth to large sizes. In particular, minor retardation of the front due to larger values of the critical size by the end of nucleation is ignored in this approximation, which becomes visible at the later times. Note that in the diffusion case the “neck” of the distribution at $r \simeq 2$ thins out with depletion, and its disappearance can be associated with the end of nucleation. In the ballistic case the “neck” is absent on the early transient stage but appears later due to depletion and associated reduction of the nucleation rate.

The QSS distributions (dashed line in Figs. 3 and 4), on the other hand, are too narrow and have a sharp rather than a continuous front, which is moving too fast. At earlier times (not shown in the figure) the QSS approximation does not reveal the subtleties of the distribution at small sizes. Otherwise, one notes that the QSS shape is reasonable and that associated numerical errors would diminish with an increasing initial barrier.

One also can access the asymptotic shape of the distribution after the nucleation is over, but before changes in R_* become essential. Introducing the dimensionless distance from the front [24] as $t_i(r) - t \simeq [r - r_i(t)]/\dot{r} = \rho$, one can write

$$f(\rho) \approx J(-\rho) \exp(-e^\rho) \quad (33)$$

with further simplification $\rho \approx (r - r_i)r_i^\theta$. In the ρ variables the shape of asymptotic distributions is thus given by mirror-

reflected nucleation curves from Figs. 1 and 2, stretched by a large dimensionless \tilde{t} , and with the sharp cutoff smoothed by the double exponential, so that the front has a width of about 1. The asymptotic shape is not expected to be approached too closely, however, since for the moderate barriers considered the condition $R_* \simeq \text{const}$ is not satisfied far enough beyond the nucleation stage, especially for $\theta = 0$.

IV. DISCUSSION

In the present study an approximate expression for time-dependent distributions of nuclei was constructed, based on distinct separation of the time scales associated with the transient nucleation and with the depletion stages. Corresponding distributions are shown in Figs. 3 and 4 for the diffusion- and ballistic-limited nucleation and growth, respectively. Those results provide a notably improved match with numerical data as compared with the traditional QSS approach, which also does not describe properly the early-time near-singular behavior of the distributions at small sizes, as well as the finite width and the double-exponential shape of the front.

The proposed non-QSS approximation is still less rigorous and slightly less accurate than the known matched asymptotic solution of the transient problem in neglect of depletion (which corresponds to early-time curves in Figs. 3 and 4), but this is justified by nonlinearity introduced by depletion. Accuracy is increased with a larger dimensionless barrier B_0 ; the errors introduced by the QSS approximation will also diminish in the limit $B_0 \rightarrow \infty$, when the two approaches eventually converge. For finite B_0 the difference between the QSS and the non-QSS descriptions is mainly determined by a dimensionless parameter $\chi = B_0 - 3 \ln n_*^0$.

In experimental situations with a not-too-large barrier the parameter χ will have only a moderate value, and non-QSS corrections will be important. This is also true for Monte Carlo and, especially for molecular dynamics computer simulations, where rather small barriers $B_0 \sim 10^1$ are often considered. The proposed solution is not expected to be too accurate for low barriers, where one could prefer numerics, but there emerges a more fundamental issue of separating the “transformed region” since for such barriers the results will be sensitive to selection of the cutoff R_0 . Formally, one could use the conservation law (9), i.e., $R_0 = 2^{1/3}$, as discussed in Sec. II B, but in that case small clusters will noticeably contribute to depletion starting from the early transient stage, and other nonconventional nucleation features can be expected.

For higher barriers, when major assumptions of the current treatment are satisfied, accuracy can be further improved by using the analytical approximation only for the nucleation flux, and treating subsequent growth numerically. That would allow to relax the condition of near-constant R_* , which is required for analytical integration of the growth equation. While this condition is justified for most of the nucleation stage, it is eventually violated, reducing the overall accuracy at large times and preventing transition to the Ostwald Ripening (OR) stage.

In a recent [11], based on a combination of analytical and numerical technique, it was shown that if the QSS nucleation description is used as initial conditions for OR, one does not observe the expected smooth, bell-shaped asymptotic distribution of LSW type [9,10]. As a possible explanation, this

was associated with the sharp front of the QSS distribution, similar to the one in Eq. (21). Smooth QSS initial distributions can be achieved by adding an external source during the nucleation stage, temporarily violating mass conservation for the system [26], which is not exactly the conventional OR situation. In that sense, the non-QSS nucleation distributions with a smooth (though narrow) front, obtained in the present study for a closed system, could provide significantly improved initial conditions for the standard OR problem, and eventually could help to resolve the issues of how fast and how closely the LSW distribution is approached. Potential importance of the nucleation transience in subsequent establishment of the LSW asymptotic regime also partly motivated the early singular perturbation solutions of the nucleation equations [14,15]. The actual description of the transition to OR stage starting from non-QSS initial conditions most likely will involve heavy numerics and will require an independent study.

Finally, one should mention limitations of the Becker-Döring approach that was used in the analysis. For example, more general coagulation-fragmentation equations can be considered [27]. In view of the above discussion, one notes that despite qualitative similarities of some of the resulting distributions, direct interactions between clusters broaden the front as compared with the BD predictions. Thus, coagulation effects too can facilitate transition to asymptotic OR (as originally suggested in Ref. [9]). Comparison with the effects of transient nucleation, however, will depend on the concrete physical system and is beyond the present work.

APPENDIX A: SECOND ITERATION FOR THE QSS APPROXIMATION

The second iteration can be written as

$$J^q(t) \simeq J_0 \exp[-\psi(x)], \quad x = t/\tilde{t}, \quad (\text{A1})$$

where the function ψ requires evaluation of the integral in the first part of Eq. (17) with $J^q(t)$ obtained from the previous step, Eq. (19). This involves

$$\int_0^x dz \exp(-z^\alpha)(x-z)^{\alpha-1},$$

which for integer θ [recall, $\alpha = (\theta + 4)/(\theta + 1)$] can be expressed in terms of a generalized hypergeometric function [28]. In the diffusion limited case $\theta = 1$ one has

$$\begin{aligned} \psi(x) = & x^{5/2} {}_5F_6 \left(\frac{1}{5}, \frac{2}{5}, \frac{3}{5}, \frac{4}{5}, 1; \frac{1}{2}, \frac{7}{10}, \frac{9}{10}, \frac{11}{10}, \frac{13}{10}, \frac{3}{2}; \frac{x^5}{4} \right) \\ & - \frac{15}{512} \pi x^5 {}_4F_5 \left(\frac{7}{10}, \frac{9}{10}, \frac{11}{10}, \frac{13}{10}; \frac{6}{5}, \frac{7}{5}, \frac{8}{5}, \frac{9}{5}, 2; \frac{x^5}{4} \right). \end{aligned} \quad (\text{A2})$$

Equation (A1) is then represented by a dashed line in Fig. 1, which after rescaling appears quite similar to the corresponding numerical curve of Ref. [13]. The asymptotes of $\psi(x)$ are given by

$$\begin{aligned} \psi(x) \sim & x^{5/2} - \frac{15\pi}{512} x^5, \quad x \rightarrow 0, \\ \psi(x) \sim & \frac{5}{2} x^{3/2} \Gamma\left(\frac{7}{5}\right) - \frac{3}{2} \Gamma\left(\frac{4}{5}\right) x^{1/2}, \quad x \rightarrow \infty, \end{aligned} \quad (\text{A3})$$

respectively. The leading $x^{5/2}$ small-time asymptote corresponds to the first iteration, where Ω_3^q [of which $\psi(x)$ is a dimensionless version] is evaluated under the assumption of a constant nucleation rate, neglecting depletion. The $x^{3/2}$ large-time asymptote indicates termination of nucleation and growth of a fixed number of particles (still, under the QSS assumption of a negligible critical size).

For $\theta = 0$ the situation is somewhat simpler:

$$\psi(x) = \frac{3E_{5/4}(x^4)}{4} + \frac{3E_{7/4}(x^4)}{4} - 3e^{-x^4} + \frac{\sqrt{2\pi}x^3}{\Gamma(\frac{3}{4})} + 4t\Gamma\left(\frac{7}{4}\right) - 1 - 3\sqrt{\pi}x^2\text{erf}(x^2), \quad (\text{A4})$$

where $E_n(z)$ are exponential integrals. The asymptotes are given by

$$\begin{aligned} \psi(x) &\sim x^4 - x^8/70, \quad x \rightarrow 0, \\ \psi(x) &\sim 4\Gamma(5/4)x^3 - 3\sqrt{\pi}x^2, \quad x \rightarrow \infty. \end{aligned} \quad (\text{A5})$$

The minor value of the small-time correction to the t^4 law [6] should be noted.

APPENDIX B: NUMERICS

The Turnbull-Fisher version of the general BD equation [29–33], modified for arbitrary type of growth was considered:

$$\begin{aligned} \frac{df_n}{dt} &= j_n - j_{n+1}, \quad j_n = \beta_{n-1}f_{n-1} - \alpha_n f_n, \\ \beta_n &= n^{(2-\theta)/3} \exp\left(\frac{W_n - W_{n+1}}{2k_B T}\right). \end{aligned} \quad (\text{B1})$$

The loss $\alpha_n = \beta_{n-1} \exp[(W_n - W_{n-1})/k_B T]$ follows from detailed balance. For the work function W_n a discrete version of $W(R)$ was used:

$$\frac{1}{k_B T} W_n = B[3(n/n_*)^{2/3} - 2n/n_*]. \quad (\text{B2})$$

The initial values $B_0 = B(0)$ and $n_*^0 = n_*(0)$ served as two independent input parameters, which fully specify the problem. The lower boundary condition was selected as $f_1 = 1$, ignoring in both the analytical and the numerical parts the minor effect of depletion. The upper boundary condition was taken as $f_n = 0$ at $n = n^{\max} + 1$, with $n^{\max} = 400$ in most runs.

The deterministic growth rate \dot{R} associated with this model is given by the generalization of the one in Ref. [29]:

$$\dot{R} = \frac{2R_*}{a\tau} \left(\frac{R_*}{R}\right)^\theta \sinh\left[\frac{a}{2}\left(1 - \frac{R_*}{R}\right)\right], \quad a = \frac{2B}{n_*} = \ln S. \quad (\text{B3})$$

For small a the difference between this rate and its continuous counterpart, Eq. (4), which was used to describe growth, is minor. This justifies the selection of a Turnbull-Fisher-type model over the original BD equations, which do not have the exponential term in the definition of β_n , and where the difference from the continuous case is much larger [34]. (The effect of discreteness on the location and width of the front is discussed, albeit without depletion, in Ref. [35], which also has earlier references.) With the above selection of β_n , the time scale τ is given by

$$\tau = \frac{3}{2B} n_*^{(\theta+4)/3} \gg 1. \quad (\text{B4})$$

The size R_0 in Eq. (10) was selected as $380^{1/3}$. This determined the depletion of monomers and the resulting increase in B and n_* , as described in the main part of the present paper. Changing R_0 to $480^{1/3}$ (with corresponding increase of the number of BD equations to 500) did not result in visible changes of the results. The numerical solution was realized in *Mathematica 7* and, except for added depletion was quite similar to the one of Ref. [16]. The time step was selected between 1 for the faster ballistic model and 5 for the slower diffusion model, respectively. Solution of the BD equations makes sense as long as the critical size is well below the upper bound. For that reason, nucleation description was terminated once R_* reached the selected R_0 . Some undercounting of the number of transformed nuclei Ω_0 can be expected upon such termination and could partly explain deviations from the analytical curve at smaller barriers in Fig. 5.

In most cases, the initial barrier and critical size were selected, respectively, as $B_0 = 25$ and $n_*^0 = 6^3 = 216$. The approximate scaling of non-QSS effects was verified for the ballistic model by selecting a larger $n_*^0 = 7^3$ and simultaneous increase of B_0 in order to keep the difference $B_0 - 3 \ln n_*^0$ fixed. The resulting shift of the nucleation curve was indeed minor, though visible. The main computational challenge came from attempts to reproduce the QSS approximation, which requires a very large barrier, leading to an increase in the number of steps needed to span the lifetime of the metastable state. For $B_0 = 40$ and the original $n_*^0 = 216$ the results indeed closely approach the QSS limit, as in Fig. 5.

[1] K. F. Kelton and A. L. Greer, *Nucleation in Condensed Matter: Applications in Materials and Biology* (Elsevier, Amsterdam, 2010).
 [2] M. Volmer and A. Weber, *Z. Phys. Chem.* **119**, 227 (1926).
 [3] L. Farkas, *Z. Phys. Chem.* **25**, 236 (1927).
 [4] R. Becker and W. Döring, *Ann. Phys.* **24**, 719 (1935).
 [5] Ya. B. Zeldovich, *Acta Physicochim URSS* **18**, 1 (1943).
 [6] A. N. Kolmogorov, *Bull. Acad. Sci. USSR (Sci. Mater. Nat.)* **3**, 3551 (1937).

[7] M. Avrami, *J. Chem. Phys.* **9**, 177 (1941).
 [8] J. W. Christian, *The Theory of Transformations in Metals and Alloys* (Pergamon Press, Oxford, 1965).
 [9] I. M. Lifshits and V. V. Slyozov, *Zh. Eksp. Teor. Fiz.* **35**, 479 (1958) [*Sov. Phys. JETP* **8**, 331 (1959)].
 [10] C. Wagner, *Z. Electrochem.* **65**, 581 (1961).
 [11] Y. Farjoun and J. C. Neu, *Phys. Rev. E* **83**, 051607 (2011).
 [12] F. M. Kuni, *Colloid J. USSR* **46**, 791 (1984).

- [13] Y. Farjoun and J. C. Neu, *Phys. Rev. E* **78**, 051402 (2008).
- [14] V. A. Shneidman, *Sov. Phys. JETP* **64**, 306 (1986).
- [15] V. A. Shneidman, *Sov. Phys. Tech. Phys.* **32**, 76 (1987).
- [16] V. A. Shneidman, *Phys. Rev. E* **82**, 031603 (2010).
- [17] L. D. Landau and E. M. Lifshitz, *Statistical Physics* (Butterworth-Heinemann, Oxford, 1980).
- [18] E. M. Lifshitz and L. P. Pitaevskii, *Physical Kinetics* (Pergamon Press, New York, 1981).
- [19] V. A. Shneidman, *Phys. Rev. Lett.* **95**, 115701 (2005).
- [20] O. Penrose, *J. Stat. Phys.* **89**, 305 (1997).
- [21] V. A. Shneidman, *Phys. Rev. Lett.* **75**, 4634 (1995).
- [22] P. G. Hill, *J. Fluid. Mech.* **25**, 593 (1966).
- [23] V. A. Shneidman, *Sov. Phys. Tech. Phys.* **33**, 1338 (1988).
- [24] V. A. Shneidman, *Phys. Rev. Lett.* **101**, 205702 (2008).
- [25] V. A. Shneidman and M. C. Weinberg, *J. Non-Cryst. Solids* **160**, 89 (1993).
- [26] V. G. Dubrovskii, M. A. Kazansky, M. V. Nazarenko, and L. T. Adzhemyan, *J. Chem. Phys.* **134**, 094507 (2011).
- [27] J. D. Gunton, M. San Miguel, P. S. Sahni, In *Phase Transitions and Critical Phenomena*, ed. C. Domb and J. L. Lebowitz (Academic, London, 1983), Vol. 8, pp. 267–482 (a review); P. Mirolid and K. Binder, *Acta Metall.* **25**, 1435 (1977); K. Binder, C. Billotet, and P. Mirolid, *Z. Phys. B* **30**, 183 (1978).
- [28] See [<http://mathworld.wolfram.com/>].
- [29] K. F. Kelton and A. L. Greer, *J. Non-Cryst. Solids* **79**, 295 (1986).
- [30] K. F. Kelton, *J. Non-Cryst. Solids* **163**, 283 (1993).
- [31] K. F. Kelton, A. L. Greer, and C. V. Thompson, *J. Chem. Phys.* **79**, 6261 (1983).
- [32] L. Granasy and P. James, *J. Chem. Phys.* **113**, 9810 (2000).
- [33] D. Turnbull and J. C. Fisher, *J. Chem. Phys.* **17**, 71 (1949).
- [34] V. A. Shneidman and M. C. Weinberg, *J. Chem. Phys.* **97**, 3629 (1992).
- [35] V. A. Shneidman, *J. Chem. Phys.* **131**, 164115 (2009).